33RD INTERNATIONAL COSMIC RAY CONFERENCE, RIO DE JANEIRO 2013
THE ASTROPARTICLE PHYSICS CONFERENCE

ICRC 2013

Study of the Crab Nebula TeV emission variability during five years with ARGO-YBJ

S.VERNETTO[1,2] FOR THE ARGO-YBJ COLLABORATION.

[1] *Osservatorio Astrofisico di Torino - INAF - Italy*
[2] *Istituto Nazionale di Fisica Nucleare - Sezione di Torino - Italy*

vernetto@to.infn.it

Abstract: The flaring activity of the Crab Nebula is one of the most puzzling phenomena of the gamma ray sky. The light curves in the energy range E >100 MeV show a high flux variability on time scales ranging from hours to weeks, with sharp emission peaks superimposed to long lasting smoother modulations, whose origin is still under debate. A long term observation of the Crab Nebula at TeV energies could add useful information to understand the mechanisms responsible of this unexpected behavior. The air shower detector ARGO-YBJ monitored the Crab Nebula in the energy range 0.5-20 TeV from November 2007 to February 2013. During the flaring episodes observed by Fermi, the average ARGO-YBJ flux is found to be a factor 2.4 $\pm$0.8 larger than the average value. Performing a long term study of the Crab Nebula flux, the ARGO-YBJ light curve is consistent with a uniform flux with a probability of 0.11. However, a comparison with the Fermi LAT light curve during 4.5 years shows a correlation between the data of the two experiments. The percent flux variations observed by ARGO-YBJ with respect to the average value are consistent with the variations of the Fermi rate, suggesting, in the hypotesis that the modulations are real, the same physical process at the origin of the observed flux variations.

Keywords: ARGO-YBJ, Gamma rays, flare, Crab Nebula

1 Introduction

The Crab Nebula is the remnant of a supernova exploded in 1054 A.D., containing a pulsar that powers a wind of relativistic particles. The interactions of these particles with the remnant gas and magnetic field produce a radiation extending from radio waves to gamma rays.

Most of the emission is attributed to synchrotron radiation of relativistic electrons and positrons. The spectral energy distribution (SED) peaks between optical and X-ray frequencies. A second component arises above 400 MeV, interpreted as Inverse Compton of the same electrons scattering off synchrotron photons and CMB photons.

The large gamma ray flux and its assumed stability, made the Crab Nebula a "standard candle" for gamma ray astronomy, suitable to calibrate instruments. Unexpectedly, on 2010 September the AGILE satellite detected a strong flare from the direction of the Crab Nebula at energies above 100 MeV, lasting 2 days, with a maximum flux 3 times larger than the average value [1], later confirmed by Fermi [2]. From then on, Fermi and AGILE reported a few more flares, characterized by a rapid increase and decay of the flux, tipically lasting a few days. The most impressive occurred on 2011 April, when the observed flux was $\sim$10 times larger than usual [3]. Besides flares, the Crab Nebula shows smaller flux variations on longer time scales, called "waves" in [4].

The origin of all these events is still under debate. The flux variations are attributed to the Nebula, since the Pulsar emission was found to be stable within 20% [3]. The measured SED shows a new spectral component emerging during flares, peaking at high energies (up to hundreds MeVs in the 2011 April flare), attributed to a synchrotron emission of a population of electrons accelerated up to energies of 10^{15} eV. The site and the origin of such a surprising activity is unknown.

In this uncertain scenario, observations at higher energies could provide useful information to shed light on the puzzle.

The ARGO-YBJ experiment is an air shower detector located at Yangbajing (Tibet, China) at an altitude of 4300 m above the sea level, devoted to gamma ray and cosmic ray studies in the TeV energy range. Due to the high duty cycle and the large field of view ($\sim$ 2 sr) ARGO-YBJ can observe every day a large part of the sky, monitoring the flux of the most luminous gamma ray sources [5, 6, 7, 8, 9]

A preliminary analysis of the data recorded by ARGO-YBJ during the flares occurences, showed an increase of the Crab flux by a factor 4-5 with a moderate statistical significance, in 3 out of 4 flares [10].

These observations have not been confirmed by Cherenkov telescopes, that could not monitor the flaring episodes because of the presence of the Moon in the night sky. Sporadic and short time measurements performed during the first part of the 2010 September flare show no evidence for a flux variability [11, 12].

In this work we present a reanalysis of the ARGO-YBJ data, focalizing the study non only during the flaring days, but on the whole observation time of the Crab Nebula (five years). The results of a correlation with Fermi data over 4.5 years are also reported.

2 The ARGO-YBJ experiment

ARGO-YBJ is an full coverage detector consisting of a $\sim$74$\times$ 78 m^2 carpet made of a single layer of Resistive Plate Chambers (RPCs) with $\sim$93% of active area, sorrounded by a partially instrumented ($\sim$20%) area up to $\sim$100$\times$110 m^2. The apparatus has a modular structure, the basic data acquisition element being a cluster (5.7$\times$7.6 m^2), made of 12 RPCs (2.85$\times$1.23 m^2). Each RPC is read

by 80 strips of $6.75\times61.8\,cm^2$ (the spatial pixels), logically organized in 10 independent pads of $55.6\times61.8\,cm^2$ which are individually acquired and represent the time pixels of the detector. The full experiment is made of 18360 pads for a total active surface of $\sim$6600m^2.

The showers firing a number of pads $N_{pad} \geq 20$ in the central carpet generate the trigger. The time of each fired pad and its location are recorded and used to reconstruct the position of the shower core and the arrival direction of the primary particle.

The angular resolution and the pointing accuracy of the detector have been evaluated by using the Moon shadow, observed by ARGO-YBJ with a statistical significance of $\sim$9 standard deviations per month. The shape of the shadow provides a measurement of the point spread function (PSF), which is in eccellent agreement with a Monte Carlo simulation [13]. The simulated angular resolution for gamma rays is smaller by $\sim$30-40% with respect to the angular resolution for cosmic rays, due to the better defined time profile of the showers.

The Moon shadow has also been used to check the absolute energy calibration of the detector, by studying the westward shift of the shadow due to the geomagnetic field. From this analysis the total absolute energy scale error, including systematics effects, is estimated to be less than 13% [13].

The full detector has been in stable data taking from 2007 November to 2013 February with a duty cycle $\sim$ 86%. The trigger rate is $\sim$3.5 kHz with a dead time of 4%.

3 Data analysis

At the ARGO-YBJ site, the Crab Nebula culminates with a zenith angle of 8° and every day is visible for 5.8 hours with a zenith angle less than 40°. The dataset used in this analysis contains all the events recorded from November 2007 to February 2013, with $N_{pad} \geq 20$, where N_{pad} is the number of hit pads on the central carpet. The total on-source time is 9520 hours.

For each source transit, the events are used to fill a set of $16^\circ\times16^\circ$ sky maps in celestial coordinates (right ascension and declination) with $0.1^\circ\times0.1^\circ$ bin size, centered on the Crab Nebula position, each map corresponding to a defined N_{pad} interval. We use 8 intervals, corresponding to N_{pad}=20-39, 40-59, 60-99, 100-199, 200-299, 300-499, 500-999 and $N_{pad} >$1000.

In this new analysis, the arrival directions of the showers have been corrected for a systematic inclination that affects the events with the core falling far from the detector center, according to the method described in [14]. The improved angular resolution increases the sensitivity by a factor 1.1, 1.3 and 1.9 for events with $N_{pad} \geq$40, 300 and 1000, respectively. For the same class of events, the radius of the opening angle that optimizes the signal-to-background ratio is 0.97°, 0.39° and 0.30°, respectively, and contains 46%, 58%, and 64% of the signal.

In order to extract the excess of γ rays, the cosmic ray background is estimated with the *time swapping* method and it is used to build the "background maps" [15].

The maps are then smoothed according to the corresponding PSF. Finally, the smoothed background map is subtracted to the smoothed event map, obtaining the "excess map", where for every bin the statistical significance of the excess is evaluated. For a detailed account of the analysis technique see [7].

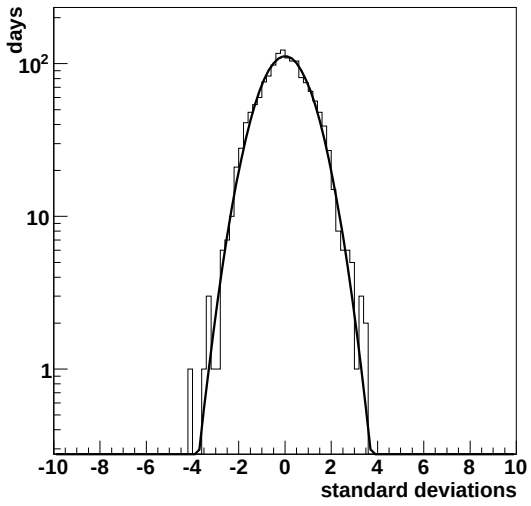

Figure 1: Distribution of the daily excesses from the Crab Nebula around the average value, in units of standard deviations, measured by ARGO-YBJ.

Adding all the transits, an excess at the source position is observed in every map, with a significance of 4.1, 7.4, 8.7, 7.0, 7.5, 6.7, 4.4 and 5.2 standard deviations, respectively, for a total significance of 19 standard deviations.

The average spectrum is evaluated by means of a simulation, by comparing the number of excess events for each N_{pad} interval, with the corresponding values expected assuming a set of test spectra. Assuming a power law spectrum, the obtained best fit in the energy range $\sim$0.5-20 TeV is: $dN/dE = 4.6\pm0.20 \times 10^{-12}(E/2\,TeV)^{-2.67\pm0.05}$ photons cm^{-2} s^{-1} TeV^{-1}, with a χ^2 of 8.1 for 6 degrees of freedom.

In order to study the time behaviour of the Crab Nebula emission, we used the events with $N_{pad} \geq$40 to avoid threshold effects. All the source transits with an observation time less than 0.5 hours have been discarded from the analysis. The total number of useful days is 1816.

Fig.1 shows the distribution of $\sigma_i=(R_i-R_m)/\delta(R_i-R_m)$, where R_i is the Crab counting rate of the i-th day, R_m is the average counting rate (R_m=18.5$\pm$1.4 ev h^{-1}), and $\delta(R_i-R_m)$ is the statistical error on the difference R_i-R_m. The daily rates are corrected for the detector efficiency and the variations of atmospheric conditions (see Subsection 4.1).

The distribution can be fitted by a Gauss function with a mean value 0.001$\pm$0.028 and r.m.s.= 1.074$\pm$0.019. The value of the r.m.s. indicates variations slighty larger than the expected statistical fluctuations.

4 Correlation with Fermi data

To study possible time correlations between ARGO-YBJ and Fermi, we used the Fermi LAT daily light curve from August 2008 to February 2013 for energy $E >$100 MeV, obtained by the authors of [4] with a standard unbinned likelihood analysis.

A Fourier spectrum of the light curve reveals a residual periodicity of 53.5 days with a semi-amplitude $\sim$7%, likely due to the LAT instrument precession [18]. This effect can be easily corrected since the oscillation is well

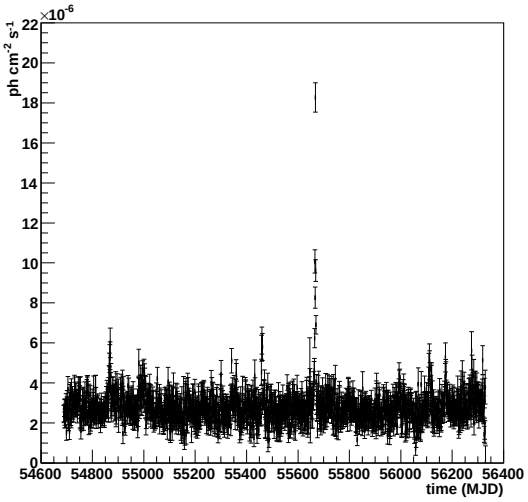

Figure 2: Crab (Nebula + Pulsar) daily light curve measured by Fermi.

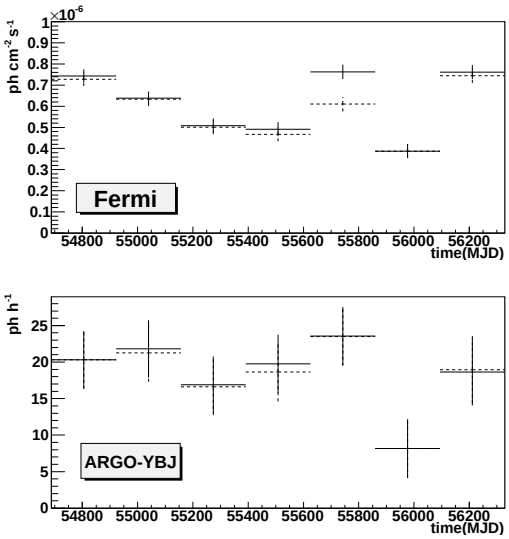

Figure 3: Upper panel: Crab Nebula flux measured by Fermi. Lower panel: Crab Nebula flux measured by ARGO-YBJ. The dashed line in both panels has been obtained excluding the days with flares.

fitted by a sinusoidal function. Fig.2 shows the corrected light curve, representing the sum of the Nebula and Pulsar fluxes. The average flux is (2.66±0.01)× 10^{-6} ph cm^{-2} s^{-1}. Even excluding the days with flares, the rate is cleary variable, with modulations on time scales of weeks and months.

Since the ARGO-YBJ sensitivity does not allow to observe a significant signal during a single flare, the Fermi data have been grouped according to the measured flux, and for any group the average ARGO-YBJ flux is evaluated. We have selected the days in which the Fermi flux is larger than F_{min}, with F_{min} ranging from 2.5 × 10^{-6} to 5.0 × 10^{-6} ph cm^{-2} s^{-1}. For any value of F_{min}, Table 1 shows the number of days satisfying this condition, and the corresponding ARGO-YBJ flux, averaged over the same days.

According to the data, the ARGO-YBJ rate increases with the the Fermi flux, indicating that there could be some correlation between the flux measured by the two detectors. During flares (here defined as the days in which the Fermi flux exceeds 5 × 10^{-6} ph cm^{-2} s^{-1}), the ARGO-YBJ flux is a factor 2.4±0.8 larger than the average value.

Fermi flux (ph cm^{-2} s^{-1})	Number of days	ARGO-YBJ rate (ph h^{-1})
>2.5 × 10^{-6}	996	18.5±1.9
>3.0 × 10^{-6}	470	19.8±2.8
>3.5 × 10^{-6}	162	23.2±4.7
>4.0 × 10^{-6}	56	32.8±8.0
>4.5 × 10^{-6}	27	34.6±11.4
>5.0 × 10^{-6}	17	44.7±14.3

Table 1: The Crab Nebula rate measured by ARGO-YBJ, for different levels of the flux measured by Fermi.

An other way to search for a time correlation is comparing the light curves of the two experiments. We rebuild the Fermi light curve using a bin width larger than 200 days in order to have a significant signal in the ARGO-YBJ data. We choose a bin width of 234 days in order to divide exactly the period from MJD 54688 (start of the Fermi data) to MJD 56328 (stop of the ARGO-YBJ data) in 7 bins.

Since the flux measured by Fermi is the sum of the Nebula and the Pulsar contributions, and since the Pulsar flux F_P averaged over the pulsation period is stable (F_P = (2.04±0.01) × 10^{-6} ph cm^{-2} s^{-1} for E >100 MeV [3]), the flux of the Pulsar has been subtracted. The obtained Nebula flux is showed in the upper panel of Fig.3. The flux shows significant variations, up to ∼40% of the average flux f_N = (6.15±0.12) × 10^{-6} ph cm^{-2} s^{-1}. The χ^2 value is 127 for 6 degrees of freedom. The large variations are not only due to flares. In the same figure the dashed curve shows the flux obtained excluding the flaring days, i.e. 17 days in which the total Crab flux exceeds 5 × 10^{-6} ph cm^{-2} s^{-1} (χ^2=101).

The lower panel of Fig.3 shows the corresponding ARGO-YBJ data. The rate mean value for this period is 18.3 ± 1.5 ev h^{-1}. The χ^2 value is 11.7. Discarding the flaring days, χ^2=11.2 (dashed curve). Even if the ARGO-YBJ rate variations are not inconsistent with statistical fluctuations (the probability of a constant flux is 0.11), the Fermi and ARGO-YBJ data seems to follow a similar trend.

Fig.4 shows the ARGO-YBJ percent rate variation with respect to the mean value (ΔF_{ARGO}) as function of the corresponding variation of the Fermi rate (ΔF_{Fermi}), for the 8 bins of the light curve.

The data appear linearly correlated. The Pearson correlation coefficient between the ARGO-YBJ and FERMI data is r=0.76.

Doing the same analysis with higher N_{pad} thresholds ($N_{pad} > 100$ and higher) no correlation is visible. The lack of correlation for more energetic events could be due the smaller statistics and to the larger fluctuations which could hidden the effect (the rate of events with $N_{pad} > 100$ is 3.2±0.4 ev h^{-1}).

Fitting the 7 points with the function $\Delta F_{ARGO} = a\,\Delta F_{Fermi} + b$, the values of the best fit parameters are a = 0.85±0.36 and b = 0.009±0.083, with χ^2=3.5 for 5 d.o.f. Discarding the flaring days, the value of the best fit parameters are a =

0.85±0.40 and b = 0.008±0.084, with χ^2=4.5. The regression coefficient $a \sim 1$ implies the same percent variation in Fermi and ARGO-YBJ rates.

4.1 Stability of the ARGO-YBJ data

Concerning the ARGO-YBJ data, the possible causes of artificial rate variations have been accurately studied in order to exclude systematic effects.

Since the measured number of events from the source $S = N - B_{ts}$ is the difference between the number of events N detected in the source observational window (that contains the source events S plus the cosmic ray background B) and the number of background events B_{ts} estimated with the time swapping method, one must analyse separately the stability of the different contributions.

1) A loss of signal events S could be produced by variations of the pointing accuracy. Studying the Moon shadow month by month, we have verified that the pointing is stable within 0.1 degree. Given the moderate angular resolution for events with $N_{pad} > 40$, such a value could produce fluctuations of the signal of less than 2%.

2) Atmospheric pressure and temperature variations can affect the detector efficiency, that can also be altered by some RPC not working properly.

3) The atmospheric conditions produce also changes in the shower rate of the order of a few percent, due to the different condition in which the showers propagate.

The two latter effects modify S, B and B_{ts} by about the same factor (neglecting the different behaviour of cosmic ray and gamma ray showers, that in this contest is a second order effect). This allows the use of B_{ts} to correct the Crab rate, multiplying the Crab flux of the i-th bin of the light curve by the correction factor $f_c = B_m/B_i$, where B_m is the average estimated background rate, and B_i is the average estimated background rate in that bin. The light curve of Fig.3 has been corrected according to this method, with f_c ranging from 0.92 to 1.08.

4) A further possible systematics could be an incorrect evaluation of the background B_{ts}. Since the value of the background is about 10^3 larger than the source signal, a small error in the background estimation could produce a large change in the source flux. We have tested the stability of the background using four fake sources located at a distance of 3 degrees from the Crab Nebula in different directions. If the background estimation was the origin of the observed flux variations, the fakes source flux would be affected by similar modulations. The light curve of the fakes source are consistent with uniform distributions with mean values consistent with zero, without any trend similar to the one observed for the Crab Nebula signal.

5 Conclusions

The ARGO-YBJ events recorded in 5 years have been reanalized to study the time variability of the Crab Nebula emission in the TeV energy range.

The ARGO-YBJ light curve is consistent with a constant flux with a probability of 0.11. However it shows modulations that appear correlated with the corresponding light curve obtained with the Fermi LAT data. According to our analysis, a percent variation of the Fermi flux corresponds to the same percent variation of the ARGO-YBJ rate, implying, in case of a real effect, a same behaviour of the gamma ray emission at energies $\sim$ 100 MeV and $\sim$1 TeV.

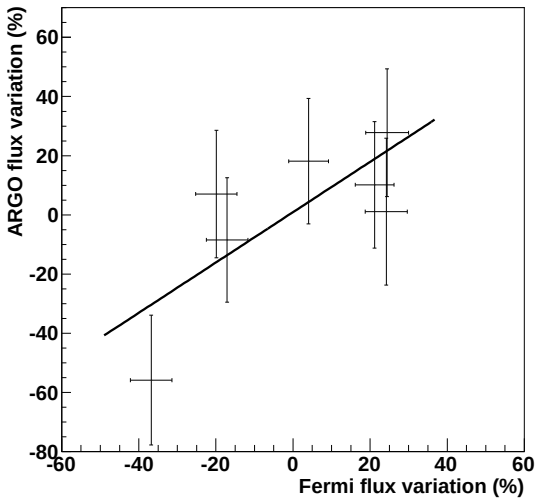

Figure 4: Percent variation of the Crab Nebula flux with respect to the average value: ARGO-YBJ vs Fermi data.

Concerning the flaring periods, the Crab Nebula flux measured by ARGO-YBJ during the days in which the Fermi flux exceeds 5×10^{-6} ph cm^{-2} s^{-1} is a factor 2.4 ±0.8 larger than the average value.

The small statistical significance of these results does not allow to claim the detection of a flux variability and requires a confirmation by more sensitive instruments. So far, no variation of the Crab Nebula flux has been reported by any detector. A TeV variable flux could hardly be interpreded as the Inverse Compton emission associated to the new synchrotron component observed during flares, and requires a new interpretation. The linearity between the Fermi and the ARGO-YBJ fluxes, and the value of the regression coefficient consistent with unity, would suggest the same physical mechanism at the origin of the flux variations observed at E$\sim$100 MeV and E$\sim$1 TeV.

Acknowledgment: We acknowledge E.Striani and M.Tavani for their kind collaboration in providing the Fermi light curve used in this analysis.

References

[1] M.Tavani et al., Science 331 (2011) 736.
[2] A.A.Abdo et al., Science 331 (2011) 739.
[3] R.Buehler et al., ApJ 749 (2012) 26.
[4] E.Striani et al., ApJ 765 (2013) 52
[5] B.Bartoli et al., ApJ 758 (2012) 2.
[6] B.Bartoli et al., ApJL 745 (2012) 22.
[7] B.Bartoli et al., ApJ 760 (2012) 110.
[8] B.Bartoli et al., ApJ 734 (2011) 110.
[9] G.Aielli et al., ApJL 714 (2010) 208.
[10] S.Vernetto et al., Nucl.Phys.B 239-240C (2013) 98.
[11] M.Mariotti et al., 2010, Astron.Telegram 2967.
[12] R.Ong et al., 2010, Astron.Telegram 2968.
[13] B.Bartoli et al., Phys. Rev. D, 84 (2011) 022003.
[14] R.Eckmann et al., Proc. 22nd ICRC, 1991, HE 3.6.16.
[15] D.R. Alexandreas et al., NIM A328 (1993) 570.
[16] F.A. Aharonian et al., A&A, 457 (2006) 899.
[17] J.Albert et al., ApJ 674 (2008) 1037.
[18] http://fermi.gsfc.nasa.gov/ssc/data/analysis/